CHAPTER V

Strain Rate Induced Crystallization in Bulk Metallic Glass Forming Liquid

Abstract

We report on the solidification of $Au_{49}Ag_{5.5}Pd_{2.3}Cu_{26.9}Si_{16.3}$ bulk metallic glass under various strain rates. Using a copper mold casting technique with a low strain rate during solidification, this alloy is capable of forming glassy rods of at least 5 mm in diameter. Surprisingly, when the liquid alloy is splat-cooled at much higher cooling rates and large strain rates, the solidified alloy is no longer fully amorphous. Our finding suggests that the large strain rate during splat-cooling induces crystallization. The pronounced difference in crystallization behavior cannot be explained by previously observed strain rate effect on viscosity alone. A strain rate induced phase separation process is suggested as one of the explanations for this crystallization behavior. Our results reveal that in order to completely characterize the intrinsic ability to form a metallic glass, a strain-rate-dependent critical cooling rate has to be considered which has significant ramifications for the processing and alloy development of bulk metallic glasses.

1. **Introduction**

In the 1950s, Turnbull predicted that glass formation in metals is possible if heterogeneous nucleation could be suppressed[1, 2]. Shortly after, Duwez and co-workers reported the synthesis of the first metallic glass[3] by rapidly cooling an Au-Si alloy at a rate of approximately 10^6 K/s. In the 1970s, ribbons, splats, powder, droplets, wires, and thin films were the typical forms of early metallic glasses obtained by rapid quenching [4-6]. Pd-Cu-Si alloy system was the first exception. Chen's discovery of this alloy system provided the first evidence that metallic glass could be cast in bulk form[7].

During the past few decades, bulk metallic glasses have been discovered in a wide range of alloys[8, 9][10-13]. In some alloys, a critical cooling rate to avoid crystallization as low as 0.005 K/s[14] and critical casting thickness of up to 7 cm were reported[15] when heterogeneous nucleation was reduced.

With the exception of some exotic BMG synthesis methods[16-19] most amorphous alloys have been created by cooling the liquid from above its liquidus temperature. In this case, the intrinsic glass forming ability (GFA) and critical casting thickness, d_{max}, were understood to be completely characterized by the critical cooling rate, R_c (see e.g. [20]).

This chapter of the thesis presents solidification studies on gold bulk metallic glass forming alloy $Au_{49}Ag_{5.5}Pd_{2.3}Cu_{26.9}Si_{16.3,}$ which could be cast into fully amorphous rods of at least 5 mm in diameter using a conventional copper mold injection method. When the liquid alloy was splat-cooled, where it was exposed to both a high cooling rate and a high strain rate, it crystallized during solidification. This suggests that the high

strain rate induces crystallization. This effect becomes less pronounced with increasing processing temperature.

2. Experimental

Ingots of $Au_{49}Ag_{5.5}Pd_{2.3}Cu_{26.9}Si_{16.3}$ alloy were prepared by arc-melting the elements (Au: 99.95%, Cu: 99.9%, Ag: 99.5%, Pd: 99.95%, Si: 99.95% purity) in a titanium-gettered, argon-filled atmosphere. Fully amorphous rectangular strips, 30 mm x 5 mm x 5 mm, were produced using a copper mold injection casting technique. The bulk glassy strips were cut into small cubic pieces of approximately 1 mm^3 in volume. Each sample was heated in a levitation coil to various temperatures ranging from 1000-1600K under 10^{-6} mbar vacuum, and then splatted into thin foils of various thicknesses using splat quencher.

The splat quencher apparatus is schematically shown in Figure V-1. First, the alloy is levitated and quickly melted inside the induction coil. Once the liquid melt reaches certain temperature (900 K and 1500 K in the present experiments), the power supply is shut off. The liquid droplet then free-fell through the induction coil due to gravity. During free-falling, the droplet passed the laser detector which triggered the time-delay unit. After some short delay time, the control unit fired the the copper piston splatters which caught the liquid droplet. During splatting, the liquid was solidified and splatted simultaneously. The droplet of approximately 1 mm diameter is splatted into foil at 20-100 microns thick. The process is completed in about 1 millisecond.

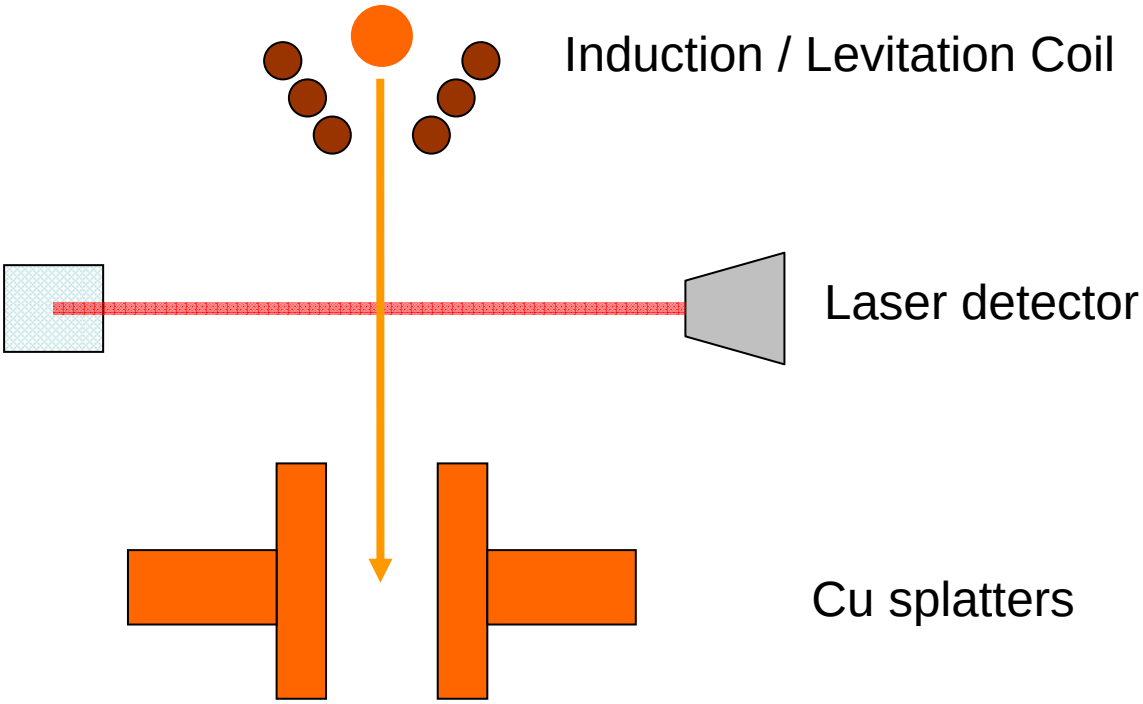

Figure V-1: Splat-quencher apparatus is schematically shown. The solid alloy is first levitated and then melted inside the induction coil. The droplet is then dropped, passing through a laser detector. The laser detector sends a time-delayed signal to the copper pistons firing unit. The droplet is then splatted from spherical shape melt into thin foil geometry.

Thermal analysis was performed in a Netzsch DSC 404c differential scanning calorimeter (DSC) and Perkin Elmer DSC7. X-ray diffraction analysis (XRD) was carried out on an Inel XRG 3000 using Cu Kα radiation.

3. Experimental Results

Figure V-2 compares the XRD spectrum of (a) a 50 micron splat-cooled sample processed at ~900K, (b) a 300 micron splat-cooled sample processed at ~900K, and (c) a

5 mm copper mold cast alloy. The spectrum of the 50 micron splat-cooled sample consists mainly of narrow peaks, indicating a substantial amount of crystallinity. The spectrum of the 300 micron splat-cooled spectrum indicates detectible amounts of crystallinity embedded in the amorphous matrix. The spectrum of the 5 mm cast sample was taken from the cross section and exhibited two broad diffraction peaks, a typical signature of a fully amorphous sample.

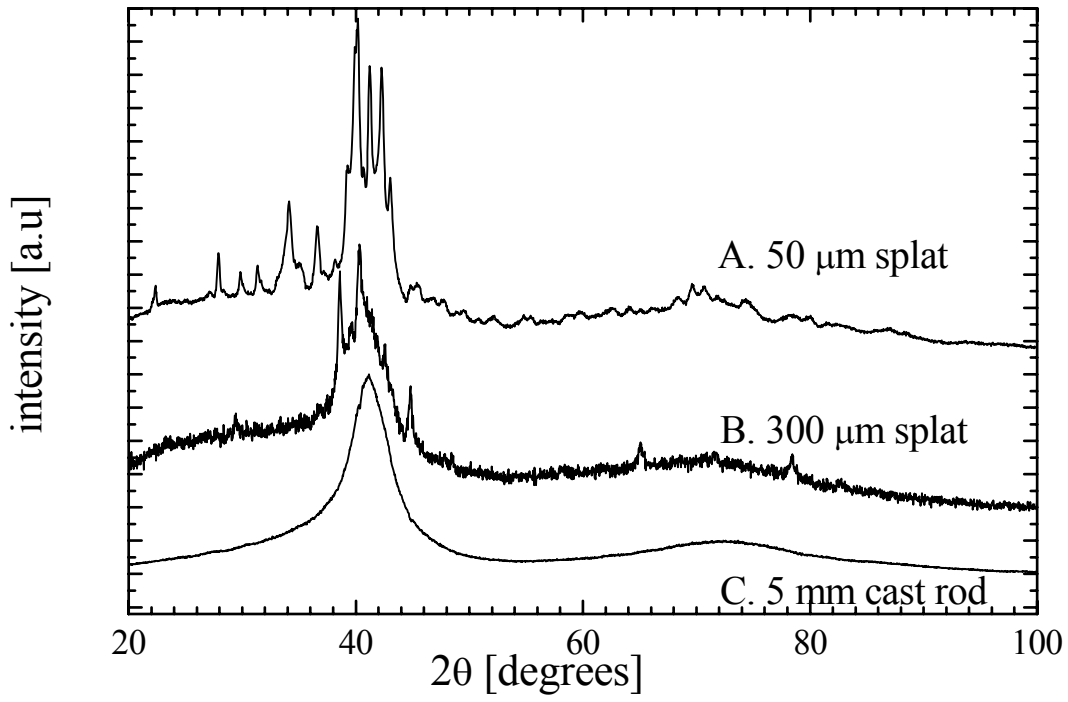

Figure V-2: X-ray diffraction spectrum for (A) 50 microns splat-cooled sample process at ~900K, (B) 300 microns splat-cooled sample process at ~900K, and (C) 5 mm cast rod processed at ~900K

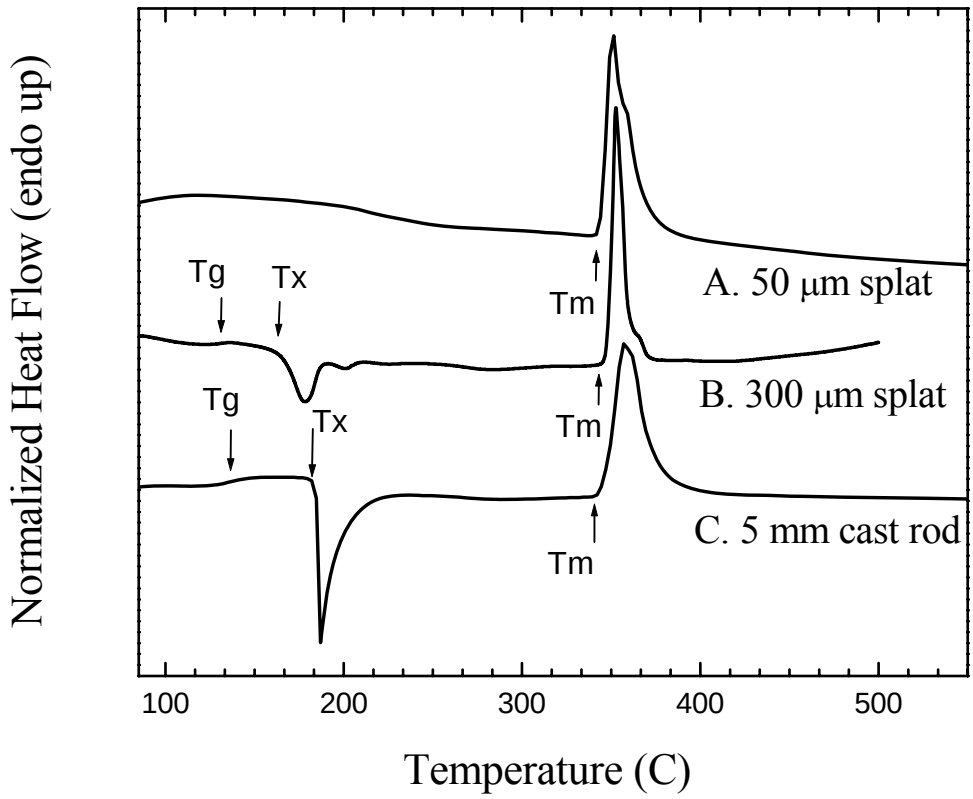

Figure V-3: Differential scanning calorimetry thermograms determined at 0.33 K/s heating rate for (A) 50 microns splat-cooled sample process at ~900K, (B) 300 microns splat-cooled sample process at ~900K, and (C) 5 mm cast rod processed at ~900K

The DSC thermograms measured while continuously heating at 0.33 K/s are shown in Figure V-3. The copper mold cast sample thermogram (c) shows a glass transition temperature, *T*g, of 403 K and a crystallization temperature, T_x, of 461 K. The ratio of the heat of crystallization to the heat of fusion is 0.75, confirming that the material was entirely amorphous[21]. The thermogram (a) of the 50 micron splat-cooled

sample does not show an obvious heat release during heating, indicating the crystalline nature of the splat. Thermogram (b) reveals the heat of crystallization to heat of fusion ratio of ~0.4, confirming that the 300 micron splat is partially crystalline. The solidification temperatures, T_m, for all three samples are in agreement with one another, implying that the nominal composition of the splat has not been altered.

To further investigate our findings the same alloy was subjected to different strain rates and processing temperatures. The results are summarized in Table V-1, V-2, and V-3. The splat foils were obtained from using the aforementioned splat quencher. The pistons' speed was varied to obtain different foil thicknesses. The cast foil of 30 microns was obtained by water quenching in thin-walled silicon molds. The millimeter-level cast strips were obtained using the injection copper mold casting technique. It was found that the crystallization was bypassed if the samples were subjected to low strain rates. The processing temperature does not have an effect on the suppression of crystallization if the strain rates are low. However, when the alloy is exposed to high strain rate (4000-10000 s^{-1})[A] crystallization occurs even though the cooling rates are in the order of 10^5-10^6 K/s[B]. This crystallization effect was found to be influenced by the processing temperature. With increasing processing temperature, the crystalline volume fraction decreases and, at about 1500 K, the sample becomes mainly amorphous.

[A] Calculated from the time required to deform a liquid drop of 1 mm diameter sphere to a splat 50 micron thick. The time is of the order of millisecond.

[B] The cooling rate is estimated from solution to the heat flow equation for a plate of liquid alloy cooled by heat conduction to a thick mold which yields $R_c^{plate} = 0.4K_tT_l / c_pL^2$ with K_t as the thermal conductivity, c_p the specific heat of the alloy, and L the plate's thickness. More information can be found in the appendix.

Sample	Cooling rate (K/s)	Processing Temperature (K)	Strain rate (s^{-1})	structure
50 μm splat foil	10^6	~900	10^4	crystalline
300 μm splat foil	$3x10^4$	~900	$4x10^3$	partially crystalline
50 μm splat foil	10^6	~1500	10^4	fully amorphous
30 μm cast foil	10^6	~900	negligible	fully amorphous
5 mm cast strip	10^2	~900	negligible	fully amorphous
5 mm cast strip	10^2	~1500	negligible	fully amorphous

Table V-1: Summary of processing parameters for $Au_{49}Ag_{5.5}Pd_{2.3}Cu_{26.9}Si_{16.3}$ alloy and the resulting structures

Cooling rate Rc / Strain rate	10^2 K/s	10^4 K/s	10^6 K/s
Negligible	**Fully Amorphous** 5 mm cast strip	**Fully Amorphous** 250 μm Cu-mold	**Fully Amorphous** 30 μm cast (Si)
10^3 s^{-1}		**Partially Amorphous** 300 μm splat	
10^4 s^{-1}			**Crystalline** 50 μm splat

Table V-2: Summary of processing parameters for $Au_{49}Ag_{5.5}Pd_{2.3}Cu_{26.9}Si_{16.3}$ alloy showing the effect of critical cooling rate (Rc) and strain rate

Processing Temp. / Strain rate	900 K	1500 K
Negligible	**Fully Amorphous** 30 μm - 5 mm cast	**Fully Amorphous** 30 μm - 5 mm cast
10^3 s^{-1}	**Partially Amorphous** 300 μm splat	**Fully Amorphous** 300 μm splat
10^4 s^{-1}	**Crystalline** 50 μm splat	**Mainly Amorphous** 50 μm splat

Table V-3: Summary of processing parameters for $Au_{49}Ag_{5.5}Pd_{2.3}Cu_{26.9}Si_{16.3}$ alloy showing the effect of processing temperatures and strain rates

4. Discussions

To date no strain rate effects on the crystallization in metallic liquid have been reported. However, for several metallic glasses, it has been found that the strain rate has an effect on the viscosity[22-25]. These non-Newtonian effects result in a decrease of the viscosity with increasing strain rate. The viscosity has a strong influence on the crystallization kinetics. According to classical nucleation theory, the time for crystallization, t_x, is proportional to[26, 27]:

$$t_x \propto \left(\frac{1}{I_{SS}\, u^3} \right)^{\frac{1}{4}}, \qquad (1)$$

where I_{ss} is the steady state nucleation rate and u the growth rate. Both I_{ss} and u are inversely proportional to the viscosity, implying $t_x \propto \eta$, which was experimentally verified by Mukherjee et al.[28]. The critical cooling rate is inversely proportional to t_x, indicating $R_c \propto 1/\eta$[28]. This implies that in order to explain the crystallization in the splat-cooled sample by the strain rate effect on viscosity, the viscosity during splat-cooling must be at least four orders of magnitude lower than the viscosity during 5 mm copper mold casting. Strain rate effects on viscosity were quantified for a Zr-based BMG by Lu et al.[29]. It was found that the strain rate effects on viscosity are most pronounced at low temperatures around T_g and become less significant as the temperature approaches T_x. For the highest temperature region studied in this work, which itself is still much lower than the expected crystallization temperature region for $Au_{49}Ag_{5.5}Pd_{2.3}Cu_{26.9}Si_{16.3}$[C],

[C] During cooling, BMGs crystallize at or above the nose in the time temperature transformation diagram, e.g., [30] J. Schroers, A. Masuhr, W. L. Johnson, R. Busch, Physical Review B 60 (1999) 11855-11858.

the viscosity dependence on strain rate is $\frac{d\log\eta}{d\log\dot{\varepsilon}}=\frac{1}{4}$. A dependence of $\frac{d\log\eta}{d\log\dot{\varepsilon}}=1$ is required to account for the experimental finding. This suggests that the observed large difference in crystallization kinetics of the differently processed samples cannot be explained by a crystallization rate enhancement due to the previously reported strain rate effect on the viscosity alone. To investigate the origin of strain-rate induced crystallization in metallic glasses, one must explore other possible influences on crystallization kinetics.

Phase separation and crystallization driven by large strain rates and related non-Newtonian liquid behavior are common in many complex fluids (see, e.g., [31-33]). The origin for strain rate effects on phase separation and crystallization in such liquids stems from the bonding nature and the size (or length) of the molecules, which is not applicable to metallic liquids. Even though many bulk metallic glass systems are known to phase separate[34-38], the relationship between strain rate effects and phase separation in metallic glass liquids has never been established.

The effect of strain rate on metallic liquid includes the effect of elastic energy storage under flow. This is considered in the Gibbs free energy, G, as an elastic energy term, E_{el}. The maximum value of this contribution can be estimated, in our case, to $E_{el}^{\max}=\frac{1}{2}\sigma_y\cdot\varepsilon_{el}$, where σ_{y} is the room temperature yield strength and $\varepsilon_{\mathrm{el}}$ is the elastic strain limit. A liquid subjected to a strain rate can release E_{el} and thereby lower its free energy by lowering its overall viscosity. Bulk metallic glass forming alloys are known to have high viscosities[39, 40], much higher than the viscosity of each of the individual elemental constituents. Therefore, it is reasonable to assume that a homogeneous BMG

forming liquid could lower its overall viscosity by phase-separating into two or more chemically distinct liquids. Such a phase separation process would then release elastic energy, and this elastic energy reduction would act as a driving force for the phase separation process. This approach to explain the influence of strain rate on the crystallization is sketched in Figure V-4.

For simplicity the composition dependence of the viscosity is assumed to be linear. Furthermore, the viscosity of the phase-separated regions are assumed to be identical. The applied strain rate during solidification phase separates the material of composition c_n into c_1 and c_2, which is driven by lowering the viscosity from η_n to η_{dec}.

The varying chemical composition of the separated regions directly influences crystallization. In particular, $Au_{49}Ag_{5.5}Pd_{2.3}Cu_{26.9}Si_{16.3}$ is known to have a strong dependence of the glass forming ability on the composition[21]. Our results imply that a phase separation process in this alloy drives the local compositions in the separated region far enough out of the glass forming composition that even a cooling rate of 10^6 K/s is insufficient to avoid crystallization.

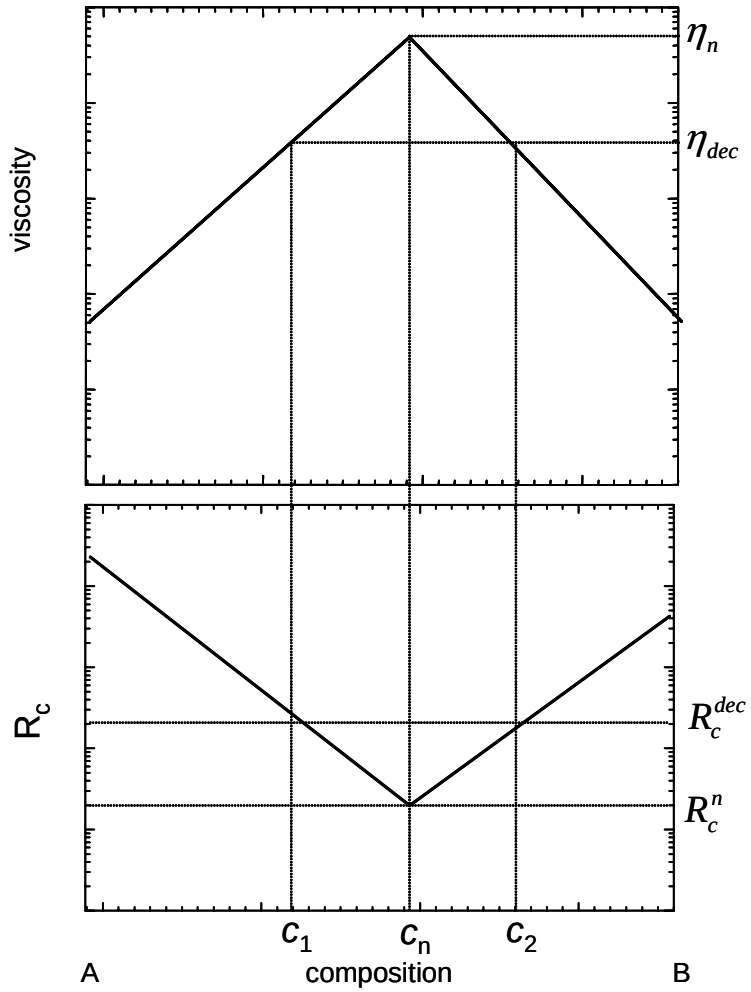

Figure V-4: Sketch of the approach to explain the influence of strain rate on the crystallization. The applied strain rate during solidification causes the material of composition c_n to phase separate into c_1 and c_2 by lowering the viscosity from η_n to η_{dec}. If the applied cooling rate is below R_c^{dec}, the material separates and crystallizes during solidification. If the applied rate is above R_c^{dec}, crystallization could be avoided during solidification, and the material only phase separates.

This scenario is sketched in the bottom part of Figure V-4. The strain rate during splat-cooling of 10^4 s^{-1} is capable of phase separating the initial composition c_n into c_1 and c_2, both with larger critical cooling rates. If now the cooling rate is below R_c^{dec} the material phase separates and crystallizes during solidification. It has been predicted[23] and observed in several systems that crystallization takes place in shear bands where plastic shear is localized[41, 42] resulting in a very high strain rate. Recent study by Lewandowski and Greer [43] suggests that the cooling rate inside the shear bands is of the order of 10^5-10^9 K/sec. Such high cooling rate could easily suppress crystallization in regular condition, i.e. strain rate is zero. Therefore the heat evolution inside the shear band could not be responsible for crystallization in solid BMGs at temperature far below Tg. The strain rate induced crystallization could very well be the explanation of such findings.

If the applied cooling rate remains larger than effective R_c^{dec}, crystallization during solidification can be avoided and the material will only phase separate during solidification. The finding by Cao et al.[44] that phase separation takes place in shear bands with no evidence of crystallization might be an example of this scenario.

The extent to which the strain rate applied during solidification of the BMG influences crystallization depends on the relative influence of the elastic energy term in comparison to the enthalpic and entropic terms in *G*. Additionally, the extent to which the composition change during phase separation affects the glass forming ability depends on the composition dependence of the glass forming ability. For example, the well-studied Zr-based and Pd-based BMGs can be expected to show a less pronounced strain rate effect on the crystallization since they possess a wide glass forming region on the

compositional space[45, 46]. In addition, the directions in the compositional space for both (i) phase separation process driven by the lowering of elastic energy and (ii) the composition sensitivity of the GFA must coincide in order to result in a strong influence of the strain rate on the crystallization kinetics. The directional concurrent between (i) and (ii) controls the degree of the strain rate effect on crystallization.

It should be mentioned that the phase separation process described in the present approach is different from the previously reported decomposition processes in metallic glasses[34-38]. In those processes, the driving force for chemical decomposition comes from a lowering of the enthalpic contribution of G. The maximum driving force for a strain rate driven decomposition process can be estimated for as $E_{el}^{\max} \approx 90$ J/mol, using $\sigma_y = 1200$ MPa and $\varepsilon_{el} = 0.015$[47]. This number is comparable to the driving force for the previously reported chemically driven decomposition process of approximately 100 J/mol[48].

Transmission electron microscope (TEM) work was completed on two splatted samples of different compositions: the best glass forming composition consisting of five elements and nominal glass forming composition consisting of four elements. For the best glass forming composition, the fully crystalline splat sample was obtained using high strain rate of 1000 /sec and 900 ºC processing temperature. TEM micrographs reveal many nano-crystals and larger particles. Crystallites of different sizes and different compositions were located at different distances from the center of the splat. For the nominal glass former, the splat is partially amorphous and the TEM micrograph of one specific area is shown in Figure V-5. Features that run across the micrograph from left to right are the remnant of microtoming which was chosen as a sample preparation method

over electro-chemical. Nanocrystals can be found along the vertical lines which may be shear bands or the strain waves that propagate through the liquid during solidification. The liquid along these lines are unstable and nanocrystals are formed.

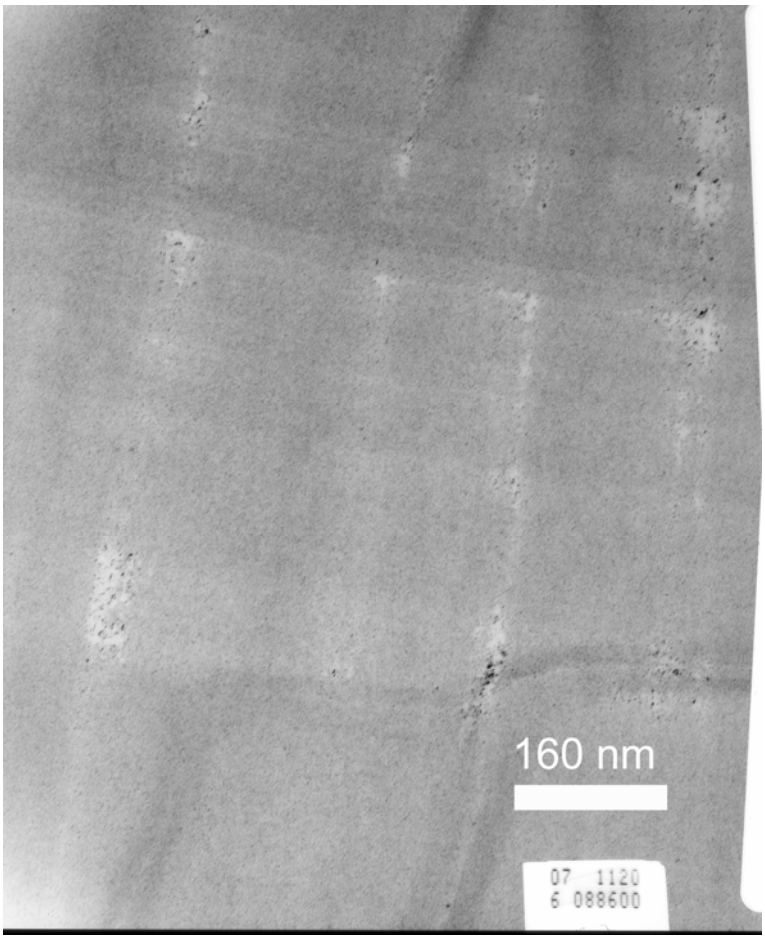

Figure V-5: Transmission electron micrograph image of partially crystalline splatted sample. The horizontal line features are the remnant of microtoming, a TEM sample preparation step. The vertical line features are decorated with nanocrystals.

5. Conclusion

The experimental evidence of a strain rate induced crystallization in a metallic system during cooling from the melt is reported. Previously reported strain rate effects on viscosity alone are not sufficient to explain this finding. A qualitative approach is suggested where the strain rate induces phase separation in the homogeneous liquid. If phase separated chemical compositions are driven out of the glass forming region for the applied cooling rate, the material crystallizes during cooling. In the present case, a cooling rate as high as 10^6 K/s is not sufficient to suppress crystallization. This work suggests the critical cooling rate must be considered in conjunction with the strain rate dependent effect in order to fully assess the intrinsic glass forming ability of metallic glass forming liquids.

References

[1] D. Turnbull, Journal of Chemical Physics 18 (1950) 769-769.

[2] D. Turnbull, M. H. Cohen, Journal of Chemical Physics 29 (1958) 1049-1054.

[3] W. Klement, R. H. Willens, P. Duwez, Nature 187 (1960) 869-870.

[4] S. A. Miller, R. J. Murphy, Journal of Metals 31 (1979) F7-F7.

[5] H. H. Liebermann, Journal of Materials Science 15 (1980) 2771-2776.

[6] F. E. Luborsky, J. L. Walter, H. H. Liebermann, E. P. Wohlfarth, Journal of Magnetism and Magnetic Materials 15-8 (1980) 1351-1354.

[7] H. S. Chen, Acta Metallurgica 22 (1974) 897-900.

[8] A. Inoue, K. Kita, T. Zhang, T. Masumoto, Materials Transactions Jim 30 (1989) 722-725.

[9] A. Inoue, T. Zhang, T. Masumoto, Materials Transactions Jim 30 (1989) 965-972.

[10] A. Peker, W. L. Johnson, Applied Physics Letters 63 (1993) 2342-2344.

[11] V. Ponnambalam, S. J. Poon, G. J. Shiflet, V. M. Keppens, R. Taylor, G. Petculescu, Applied Physics Letters 83 (2003) 1131-1133.

[12] J. Schroers, W. L. Johnson, Applied Physics Letters 84 (2004) 3666-3668.

[13] D. H. Xu, B. Lohwongwatana, G. Duan, W. L. Johnson, C. Garland, Acta Materialia 52 (2004) 2621-2624.

[14] J. Schroers, W. L. Johnson, Metastable, Mechanically Alloyed and Nanocrystalline Materials 386-3 (2002) 111-115.

[15] A. Inoue, N. Nishiyama, H. Kimura, Materials Transactions Jim 38 (1997) 179-183.

[16] M. C. Lee, J. M. Kendall, W. L. Johnson, Applied Physics Letters 40 (1982) 382-384.

[17] X. L. Yeh, K. Samwer, W. L. Johnson, Applied Physics Letters 42 (1983) 242-244.

[18] M. Vonallmen, E. Huber, A. Blatter, K. Affolter, International Journal of Rapid Solidification 1 (1984) 15-25.

[19] A. Blatter, M. Vonallmen, Physical Review Letters 54 (1985) 2103-2106.

[20] A. Inoue, Acta Materialia 48 (2000) 279-306.

[21] J. Schroers, B. Lohwongwatana, W. L. Johnson, A. Peker, Applied Physics Letters 87 (2005) -.

[22] F. Spaepen, Acta Metallurgica 25 (1977) 407-415.

[23] A. S. Argon, Acta Metallurgica 27 (1979) 47-58.

[24] Y. Kawamura, H. Kato, A. Inoue, T. Masumoto, Materials Science and Engineering a-Structural Materials Properties Microstructure and Processing 219 (1996) 39-43.

[25] T. G. Nieh, C. Schuh, J. Wadsworth, Y. Li, Intermetallics 10 (2002) 1177-1182.

[26] D. R. Uhlmann, Journal of Non-Crystalline Solids 25 (1977) 42-85.

[27] D. R. Uhlmann, Journal of Non-Crystalline Solids 41 (1980) 347-357.

[28] S. Mukherjee, J. Schroers, W. L. Johnson, W. K. Rhim, Physical Review Letters 94 (2005) -.

[29] J. Lu, G. Ravichandran, W. L. Johnson, Acta Materialia 51 (2003) 3429-3443.

[30] J. Schroers, A. Masuhr, W. L. Johnson, R. Busch, Physical Review B 60 (1999) 11855-11858.

[31] J. H. Han, C. D. Han, Journal of Polymer Science Part B-Polymer Physics 28 (1990) 711-741.

[32] J. H. Han, C. D. Han, Journal of Polymer Science Part B-Polymer Physics 28 (1990) 743-761.

[33] C. R. Safinya, E. B. Sirota, R. J. Plano, Physical Review Letters 66 (1991) 1986-1989.

[34] R. Busch, S. Schneider, A. Peker, W. L. Johnson, Applied Physics Letters 67 (1995) 1544-1546.

[35] M. P. Macht, N. Wanderka, A. Wiedenmann, H. Wollenberger, Q. Wei, H. J. Fecht, S. G. Klose, Metastable, Mechanically Alloyed and Nanocrystalline Materials, Pts 1 and 2 225 (1996) 65-70.

[36] J. F. Loffler, W. L. Johnson, Materials Science and Engineering a-Structural Materials Properties Microstructure and Processing 304 (2001) 670-673.

[37] M. K. Miller, T. D. Shen, R. B. Schwarz, Intermetallics 10 (2002) 1047-1052.

[38] A. A. Kundig, M. Ohnuma, D. H. Ping, T. Ohkubo, K. Hono, Acta Materialia 52 (2004) 2441-2448.

[39] L. Shadowspeaker, R. Busch, Applied Physics Letters 85 (2004) 2508-2510.

[40] S. Mukherjee, J. Schroers, Z. Zhou, W. L. Johnson, W. K. Rhim, Acta Materialia 52 (2004) 3689-3695.

[41] H. Chen, Y. He, G. J. Shiflet, S. J. Poon, Nature 367 (1994) 541-543.

[42] J. J. Kim, Y. Choi, S. Suresh, A. S. Argon, Science 295 (2002) 654-657.

[43] J. J. Lewandowski, A. L. Greer, Nature Materials 5 (2006) 15-18.

[44] Q. P. Cao, J. F. Li, Y. H. Zhou, J. Z. Jiang, Applied Physics Letters 86 (2005) -.

[45] T. D. Shen, Y. He, R. B. Schwarz, Journal of Materials Research 14 (1999) 2107-2115.

[46] T. A. Waniuk, J. Schroers, W. L. Johnson, Applied Physics Letters 78 (2001) 1213-1215.

[47] B. Lohwongwatana, J. Schroers, W. L. Johnson, Hard 18K and .850 Pt Alloys That Can Be Processed Like Plastics or Blown Like Glass, in: Santa Fe Symposium, Arbuquerque, NM, 2007.

[48] Y. J. Kim, R. Busch, W. L. Johnson, A. J. Rulison, W. K. Rhim, Applied Physics Letters 68 (1996) 1057-1059.